Final Report for AOARD Grant *FA2386-10-1-4080*

Photophysical Properties on Functional π-electronic Molecular Systems

August 2012

Principal Investigators: Prof. Dongho Kim

E-mail Address: dongho@yonsei.ac.kr

Institution: Spectroscopy Laboratory for Functional π-Electronic Systems and Department of Chemistry, Yonsei University, Seoul 120-749, Korea

Mailing Address: 134 Shinchon-dong, Seodaemun-gu, Seoul 120-749, Korea

Phone: +82-2-2123-2436

Fax: +82-2-2123-2434

Period of Performance: 01/10/2011 – 30/09/2012

Report Documentation Page

Form Approved
OMB No. 0704-0188

Public reporting burden for the collection of information is estimated to average 1 hour per response, including the time for reviewing instructions, searching existing data sources, gathering and maintaining the data needed, and completing and reviewing the collection of information. Send comments regarding this burden estimate or any other aspect of this collection of information, including suggestions for reducing this burden, to Washington Headquarters Services, Directorate for Information Operations and Reports, 1215 Jefferson Davis Highway, Suite 1204, Arlington VA 22202-4302. Respondents should be aware that notwithstanding any other provision of law, no person shall be subject to a penalty for failing to comply with a collection of information if it does not display a currently valid OMB control number.

1. REPORT DATE	2. REPORT TYPE	3. DATES COVERED
06 SEP 2012	**Final**	**26-08-2011 to 25-08-2012**

4. TITLE AND SUBTITLE
Photophysical Properties on Functional Pi-Electronic Molecular Systems

5a. CONTRACT NUMBER
FA23861114060

5b. GRANT NUMBER

5c. PROGRAM ELEMENT NUMBER

6. AUTHOR(S)
Dongho Kim

5d. PROJECT NUMBER

5e. TASK NUMBER

5f. WORK UNIT NUMBER

7. PERFORMING ORGANIZATION NAME(S) AND ADDRESS(ES)
Yonsei University,Shinchon-Dong 134, Seodaemoon-Ku,Seoul 120-749,Korea (South),KR,120749

8. PERFORMING ORGANIZATION REPORT NUMBER
N/A

9. SPONSORING/MONITORING AGENCY NAME(S) AND ADDRESS(ES)
AOARD, UNIT 45002, APO, AP, 96338-5002

10. SPONSOR/MONITOR'S ACRONYM(S)
AOARD

11. SPONSOR/MONITOR'S REPORT NUMBER(S)
AOARD-114060

12. DISTRIBUTION/AVAILABILITY STATEMENT
Approved for public release; distribution unlimited

13. SUPPLEMENTARY NOTES

14. ABSTRACT
The researchers have investigated the photophysical properties of various porphyrinoids such as expanded porphyrins, hybrid porphyrin tapes, etc. using theoretical calculations and various spectroscopic methodologies in conjunction with the topology transformation between aromatic and antiaromatic porphyrinoids by conformational changes via kinetic and thermodynamic control, etc. Especially, they have been interested in their nonlinear optical properties of H?ckel/M?bius aromatic and antiaromatic expanded porphyrins based on the comparison of the two-photon absorption cross section spectra.

15. SUBJECT TERMS
Materials Characterization, Materials Chemistry, Nonlinear Optical Materials, Spectroscopy

16. SECURITY CLASSIFICATION OF:			17. LIMITATION OF ABSTRACT	18. NUMBER OF PAGES	19a. NAME OF RESPONSIBLE PERSON
a. REPORT	b. ABSTRACT	c. THIS PAGE			
unclassified	**unclassified**	**unclassified**	**Same as Report (SAR)**	**23**	

Table of Contents

Abstract

In this report for AFSOR/AOARD project (*FA2386-10-1-4080*), we have investigated the photophysical properties of various porphyrinoids such as expanded porphyrins, hybrid porphyrin tapes, *etc*. using theoretical calculations and various spectroscopic methodologies in conjunction with the topology transformation between aromatic and antiaromatic porphyrinoids by conformational changes via kinetic and thermodynamic control, *etc*. Especially, we have been interested in their nonlinear optical properties of Hückel/Möbius aromatic and antiaromatic expanded porphyrins based on the comparison of the two-photon absorption cross section spectra.

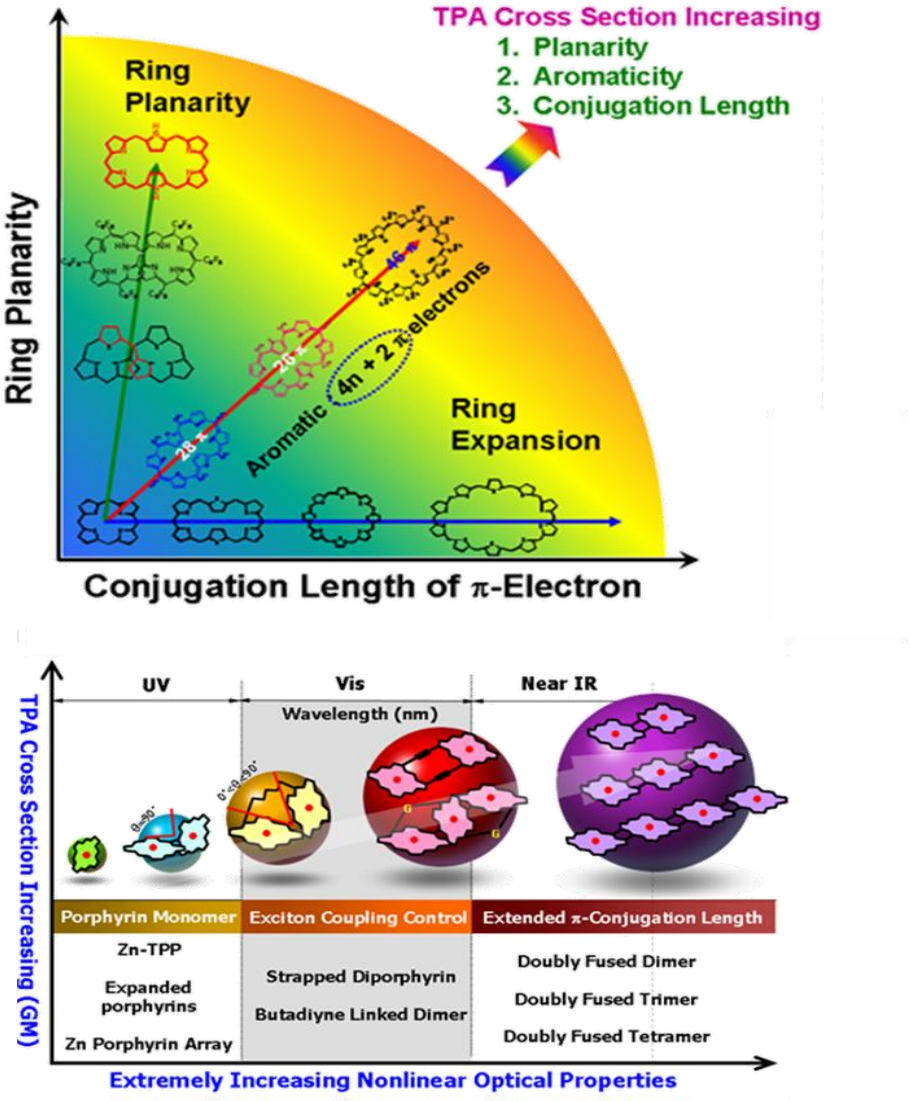

Figure 1. Molecular design strategies of various porphyrinoids for enhanced nonlinear properties.

Introduction

Aromaticity is one of the most intriguing concepts in organic chemistry. It has recently witnessed a renaissance with the appearance of conceptually new structures, including Möbius topological aromatic molecules, metal d-electron-mediated aromatic complexes, spherical shaped three-dimensional models, and so on. Also extensive efforts have been continuously devoted to the exploration of π-conjugated porphyrins in light of their possible applications, such as organic semiconductors, photodynamic therapy (PDT), nonlinear optics (NLO), photovoltaics, and so forth.

Hückel's [4n+2/4n]π rule represents one of the most successful approaches to rationalizing aromaticity from a theoretical point of view. According to this rule, a flat monocyclic system with [4n+2]π-electrons is aromatic, whereas a planar system with [4n]π-electrons is antiaromatic. To date, the majority of aromatic molecules subject to detailed analysis have consisted of closed-shell cyclic systems.

In contrast, the study of aromaticity effects in molecules with open-shell electronic states is still in its infancy. The concept of open-shell aromaticity was predicted by Baird, who suggested that [4n]π annulenes in their triplet π-π* states would display aromatic character, whereas low symmetry [4n+2]π triplet species would prove to be antiaromatic. Subsequently, numerous theoretical studies have provided a support for the notion that [4n]π annulene systems would be aromatic in their triplet states.

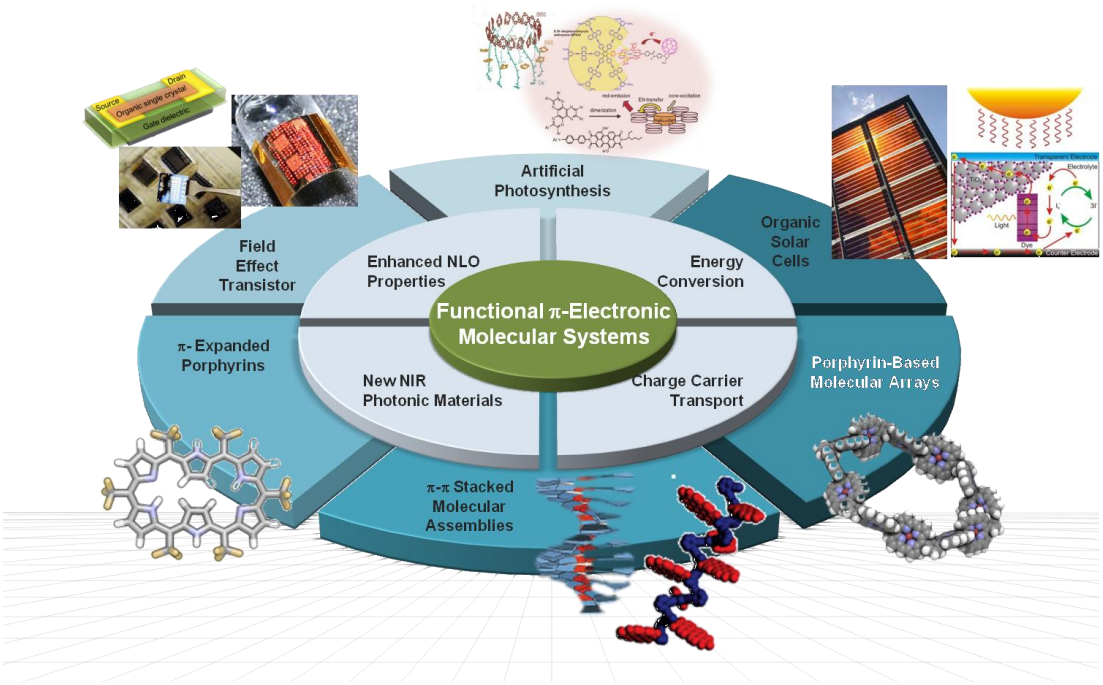

Figure 2. Executive summary of the proposed research

Porphyrins and their analogues (porphyrinoids) are particularly attractive molecules for exploration of various types of aromaticity, because most porphyrinoids possess circular conjugation pathways in their macrocyclic ring with various molecular structures. π-electron delocalization and aromaticity in porphyrinoids are strongly affected by i) structural modifications and ii) redox chemistry, etc. Furthermore, this aromaticity has a strong influence on the spectroscopic properties and chemical reactivity of porphyrinoids. In this context, considerable efforts have been devoted to exploring and understanding the relationship between aromaticity and spectroscopic properties in a variety of aromatic and antiaromatic porphyrinoids.

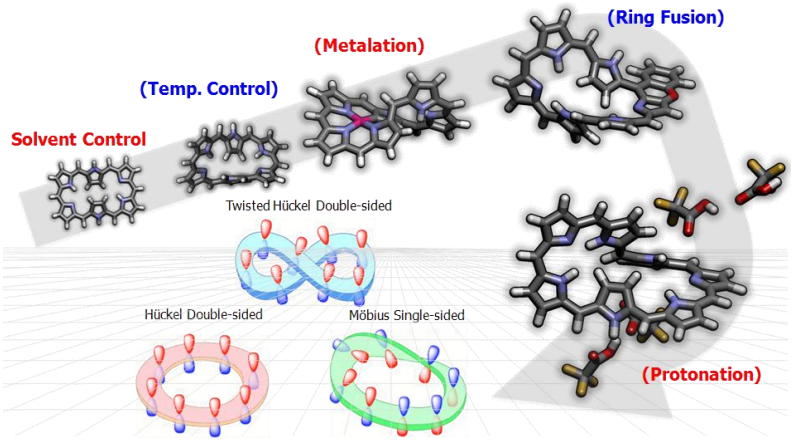

Figure 3. Examples of aromaticity control for expanded porphryins

Thus, a series of various porphyrinoids are in the limelight being expected to shed light on this field because they have some advantages to study the aromaticity; i) it is possible to control the number of conjugated π-electrons by changing the number of connected pyrrole rings, ii) by providing a comparable set of [4n]/[4n+2]π molecular systems through a facile two-electron reduction/oxidation process, the systematic investigations are easily accessible, satisfying the prerequisites that only the number of π-electrons has to be different with the same structure and chemical environment, and iii) above all, it is easy to change the molecular conformations by both synthetic and non-synthetic ways. Again, it should be noted that the topology control is an important factor in assessing the structure-property relationship. In this regard, various attempts to modify the overall structures of porphyrinoids have been made by temperature control, solvent changes, and functional group modifications (Figure 3). With these active control methods of molecular topologies in hand, the structure-property relationship of porphyrinoids in conjunction with aromaticity has been vigorously explored by using ultrafast spectroscopic measurements as well as theoretical calculations.

Methodologies

(1) Experimental Method

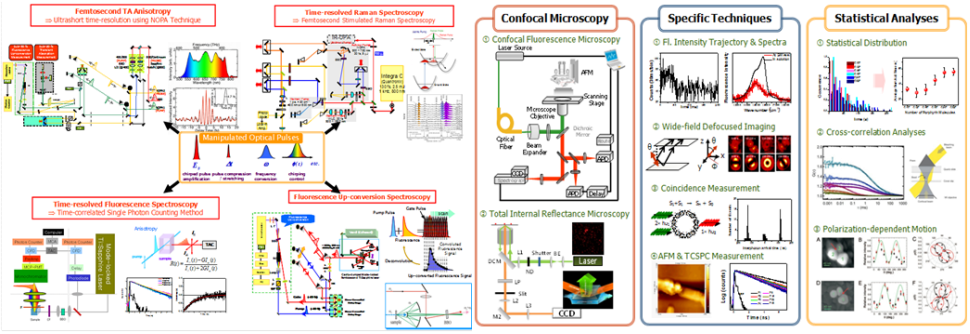

① Steady-State Laser Spectroscopy

- •Laser-Induced Luminescence Spectroscopy
- •Resonance Raman Spectroscopy

② Time-Resolved Laser Spectroscopy

- •Nanosecond Flash Photolysis
- •Picosecond Time-Correlated Single Photon Counting (TCSPC) Method
- •Vis/IR Femtosecond Transient Absorption Spectroscopy
- •Femtosecond Fluorescence Up-Conversion Spectroscopy

③ Non-Linear Spectroscopy

- •Femtosecond Z-Scan Method

(2) Quantum Mechanical Calculation

- • Nuclear-Independent Chemical Shift (**NICS**) Values
- • Anisotropy of the Induced Current Density (**AICD**) Calculation
- • Molecular Orbitals & Electronic Excited-State Excitation Energies

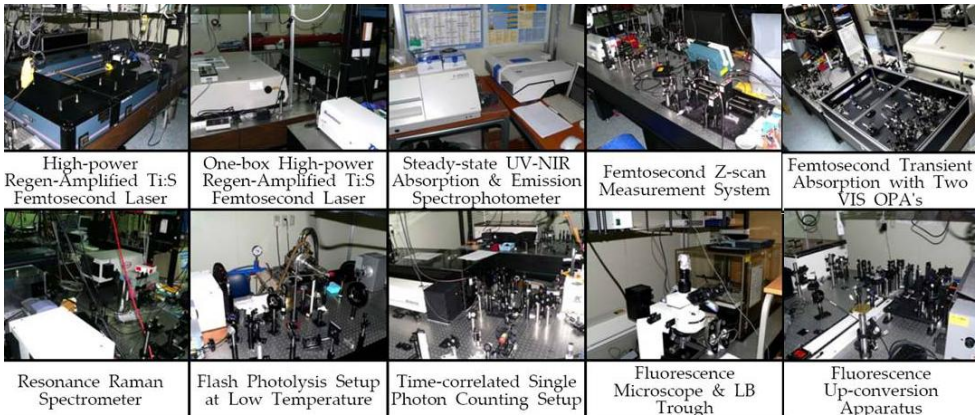

Results and Discussion

(1) Hybrid porphyrin tapes

Organic compounds with large TPA cross-sections are of general interest due to their numerous potential applications in 3D micro fabrication, optical storage, optical-limiting devices, photodynamic therapy, and so on. Extensive studies have been carried out to elucidate the molecular structure–TPA property relationship. Basically, the most important factor for the enhancement of TPA property is likely to be the extension of π-electron conjugation. For example, meso-butadiyne-linked oligoporphyrins nicely illustrate the dependency on the number of porphyrin units, exhibiting TPA cross-section values of 20 GM for monomer, 9100 GM for dimer, and 22000 GM for tetramer. In this aspect, porphyrin tapes are promising, because they have a completely planar structure and an extended π-conjugated system. We have already reported extremely large TPA values for porphyrin tape dimer, trimer, and tetramer consisting of 4-nonylphenyl and 3,5-ditert-butylphenyl-substituted porphyrins as 11900, 18500, and 41200 GM, respectively, which were obtained by photoexcitation at 1200, 2300 and 2300 nm, respectively. In this report, we have measured the TPA values of the series of meso-meso, *β–β, β–β* triply linked porphyrin dimers and trimers with 3,5-di-tert-butylphenyl-substituted donor-type (D) and pentafluorophenyl-substituted acceptor-type (A) porphyrin as the constituent moieties by using a wavelength-scanning open-aperture Z-scan method, with NIR pulses generated from an NIR optical parametric amplifier pumped by a femtosecond Ti:sapphire regenerative amplifier system with a 130 fs pulse width. We have measured the TPA values by photoexcitation in the wavelength range from 1650 to 2400 nm at which the one-photon absorption contribution is negligible and since it would be very difficult to measure correct TPA values by photoexcitation shorter than 1650 nm due to a non-negligible one-photon absorption contribution. The TPA spectra largely follow the one-photon absorption spectra at near Q- and B-band regions. In the case of **1** and **2**, the maximum TPA cross-section values were measured to be 1900 and 21000 GM respectively, in which the TPA value per porphyrin units of **2** is about seven times larger than that of dimer **1**, reflecting that the TPA values are strongly associated with the effective π-conjugation length. With regard to the NLO properties of hybrid porphyrin tapes **3**–**6**, it should be considered that large molecular polarizability is known to be another important factor which contributes to a large TPA cross-section value. Since the pioneering work by Marder, Perry, and co-workers in 1997, many efforts have been directed for enhancing the TPA by using donor(D)/acceptor(A)-type

multichromophoric systems, introducing additional groups to perturb the charge redistribution, and elongating the effective π-conjugation length. In terms of the molecular symmetry, a quadrapolar chromophore (D-π-A-π-D) is more likely to afford a larger TPA value than that of a dipolar chromophore (D-π-A). Actually, the TPA values of D-A dimer **3** and D-A-D trimer **4** were determined to be 2200 and 27000 GM, respectively. Compared with dimer **1** (D-D) and trimer **2** (D-DD), the TPA values of D-A-D trimer **4** exhibited enhancement in the TPA properties, while D-A dimer **2** showed little enhancement. Similarly, D-A-D trimers **5** and **6** exhibited TPA values of 24000 and 26000 GM, respectively, by photoexcitation at 1700 nm. Among the three D-A-D trimers, the highest TPA value in **4** may be rationalized in terms of the smallest HOMO–LUMO gap. On the other hand, the difference between **5** and **6** probably arises from the electronic nature of central acceptor-type porphyrin unit, since free-base porphyrin is more electron-deficient than Zn(II)–porphyrin and thus enhances the D-A-D character. We can conclude that the combination of π-conjugation elongation as well as a D-A-D strategy for triply linked porphyrin trimers definitely improves the overall TPA properties, while the effect of π-conjugation is a dominant contribution to the enhancement of TPA properties.

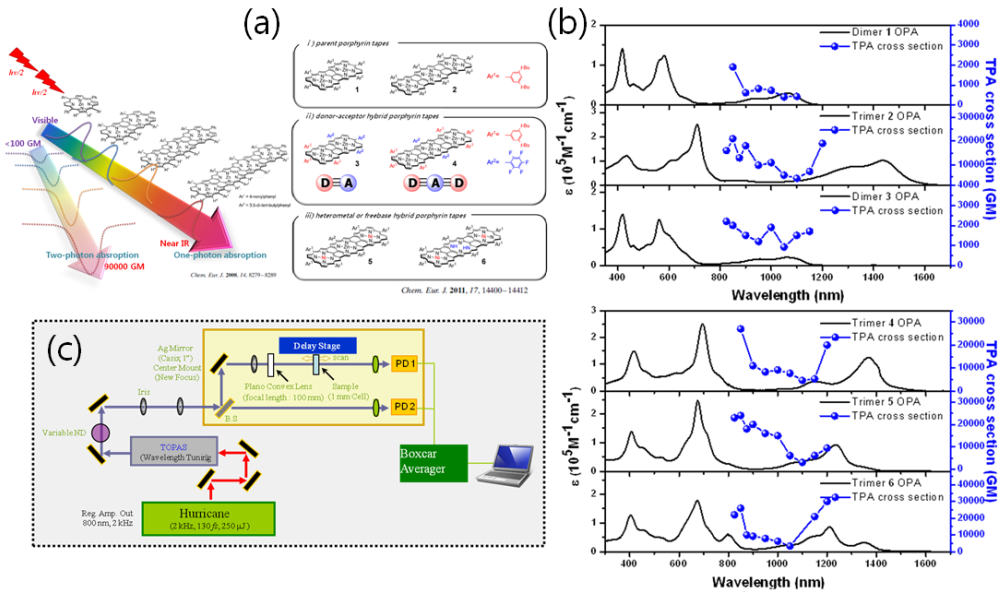

Figure 4. (a) Porphyrin tapes studied in this article. (b) One-photon absorption (black) and TPA spectrum (blue) (c) TPA laser setup.

(b) Hexaphyrin Fused to Two Anthracenes

One of the current topics in porphyrin chemistry is the synthesis of highly conjugated porphyrins that exhibit absorption bands reaching into the near infrared (NIR) region and a large range of nonlinear optical properties; such molecules are promising in the fields of organic semiconductors and photovoltaics, two-photon excited photodynamic therapy, and all-optical processing. Effective synthetic strategies are to bridge porphyrins with a conjugative linker, to directly fuse porphyrins, and to fuse aromatic segments to the porphyrin periphery. Conjugated porphyrins prepared by these strategies exhibit strongly perturbed optical and electronic properties, thus reflecting the flexible electronic nature of porphyrins. Anderson and co-workers have demonstrated that the fusion of anthracene is effective in the expansion of the conjugated network of porphyrins by exploring porphyrins fused to one, two, and four anthracenes, all of which display highly red-shifted Q bands (λ_{max}=855, 973, and 1417 nm, respectively). In recent years, expanded porphyrins have emerged as new functional chromophores, which encompass larger conjugated networks and are electronically more flexible than porphyrins. In this sense, these expanded porphyrins may be more promising as a component of highly conjugated chromophores, when fused with appropriate aromatic segments.

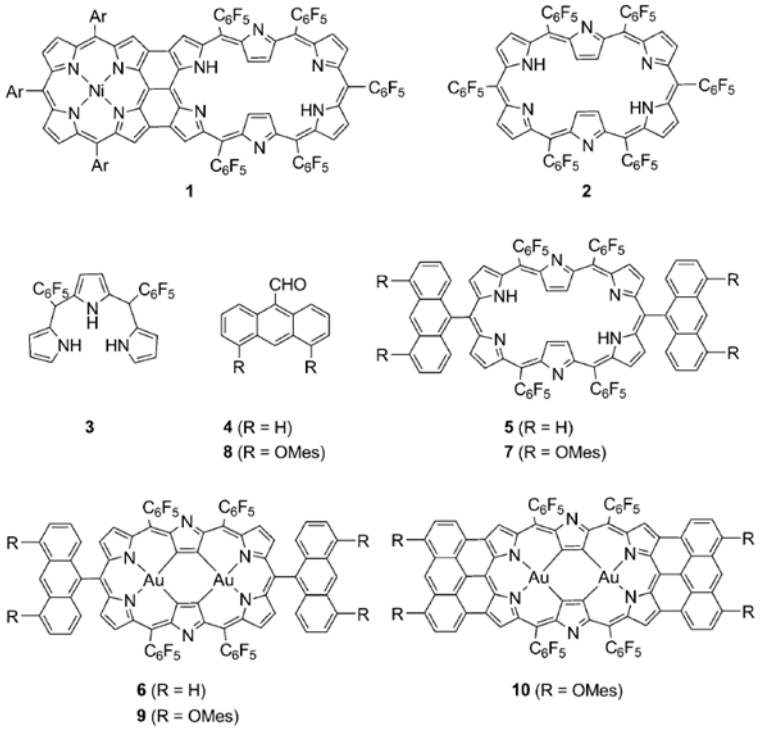

Scheme 1. Substrates and hexaphyrin derivatives. Ar=3,5-di-tert-butylphenyl, Mes=mesityl.

Despite this potential, except for porphyrin-fused hexaphyrins **1** (Scheme 1), the peripheral fusion reactions of expanded porphyrins have been rarely studied, largely because of synthetic difficulties. We envisioned that the fusion of anthracenes to rectangular hexaphyrins, such as **2**, would be feasible, because their short sides are similar in length to the long side of anthracene, and the resultant anthracenefused [26]hexaphyrins would show highly perturbed optical and electrochemical properties. Herein, we report the synthesis of **10**, a [26]hexaphyrin fused to two anthracenes, which exhibits an extensively red-shifted and sharp absorption band reaching into NIR region, and multiple reversible redox potentials.

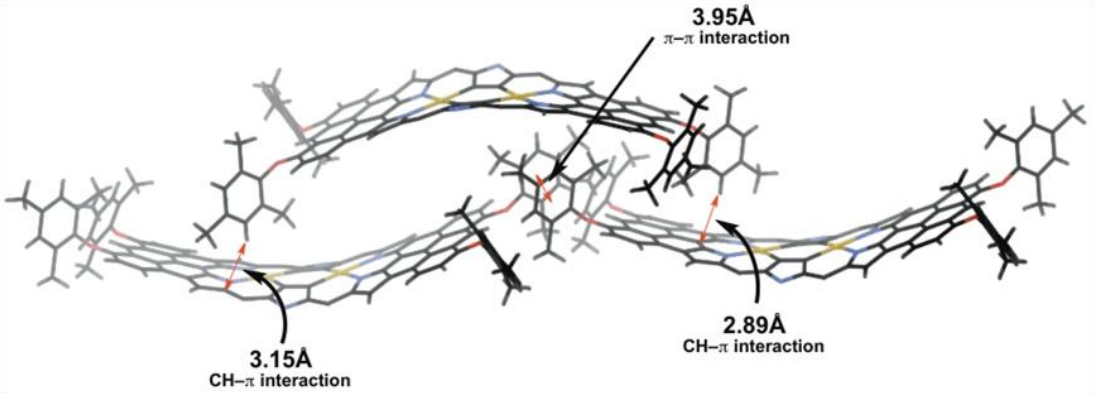

Figuer 5. Partial packing structure of **10.**

The unambiguous structural determination of **10** was obtained by X-ray analysis. Crystals of **10** were grown by allowing hexane vapor to diffuse into its CH_2Cl_2 solution. Compound **10** displays a remarkably elongated, rectangular (7.28 x 19.94 Å), almost planar structure; the dihedral angle of the two anthracene segments is 141.38. In the crystal-packing structure of **10**, an infinite molecular network is observed, and features an alternate packing arrangement wherein two molecules are positioned in an offset manner with their concave sides facing each other so that half the molecule overlaps (Figure 5). This arrangement is held by favorable CH/π interactions between the mesityloxy substituents and hexaphyrin. Figure 6 shows the absorption spectra of solutions of **9** and **10** in CH_2Cl_2. The bis(Au^{III}) hexaphyrin

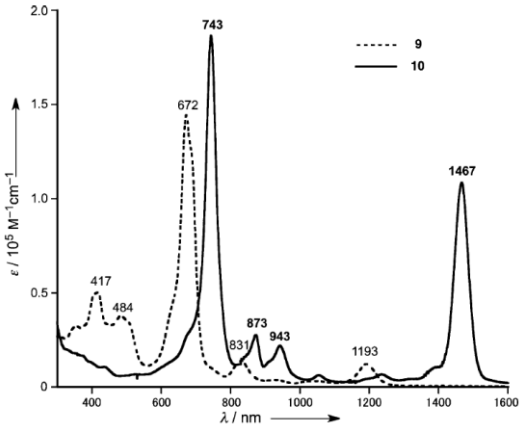

Figure 6. UV/Vis/NIR absorption spectra of **9** and **10** in CH_2Cl_2

complex **9** exhibits a slightly split Soret-like band at 672 nm, which is red-shifted from that of **7** by 96 nm, and Q-band-like bands at 831 and 1193 nm. These spectral features are common for bis(Au^{III}) hexaphyrins, as reported previously. The absorption spectrum of **10** exhibits a red-shifted and intensified Soret-like band at 743 nm and Q-band-like bands at 873, 943, and 1467 nm. Of these bands, the most red-shifted band is remarkably sharp and intensified (optical HOMO–LUMO gap; 0.84 eV, fwhm=223 cm^{-1}). These absorption characteristics originate from the elongated conjugation along the long molecular axis of **10**.

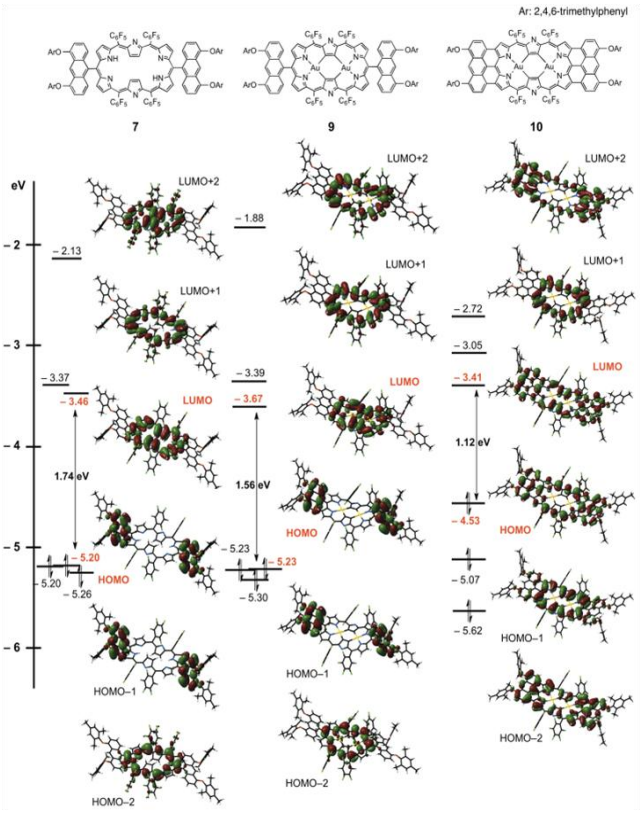

Figure 7. MO diagrams of **7**, **9**, and **10**.

Third-order nonlinear optical (NLO) responses of **9** and **10** are also of interest in view of their extended π-conjugation pathways through fused anthracene units. Two-photon absorption (TPA) measurements were conducted for **9** and **10** by using a wavelength-scanning open-aperture Z-scan method in the wavelength region ranging from 1400 to 2400 nm and from 1700 to 2400 nm, respectively, where one-photon absorption contribution is negligible (Figure 8). It was difficult to measure accurate TPA values by photoexcitations shorter than 1400 for **9**, and 1700 nm for **10**. Bis(AuIII) hexaphyrin complex **9** showed the maximum TPA cross section value of 2500 GM by photoexcitation at 1700 nm, whereas anthracene- fused [26]hexaphyrin **10** exhibited the maximum value of 7600 GM by photoexcitation at the same wavelength. The much higher value for **10** compared to that for **9** can be explained by the extended π-conjugation in **10**. Furthermore, both **9** and **10** compounds showed larger TPA values than hexakis(pentafluorophenyl) substituted [26]hexaphyrin **2** (ca. 1000 GM). This result can be explained by the effect structural changes can have on donor(D)/acceptor(A)-type multichromophoric systems: the introduction of electron-rich anthryl substituents and electron-deficient pentafluorophenyl substituents perturbs the charge redistribution, and

elongates the effective π-conjugation length. We can conclude that a combination of elongation of the π-conjugation, as well as D/A perturbation to hexaphyrin improves the overall TPA properties.

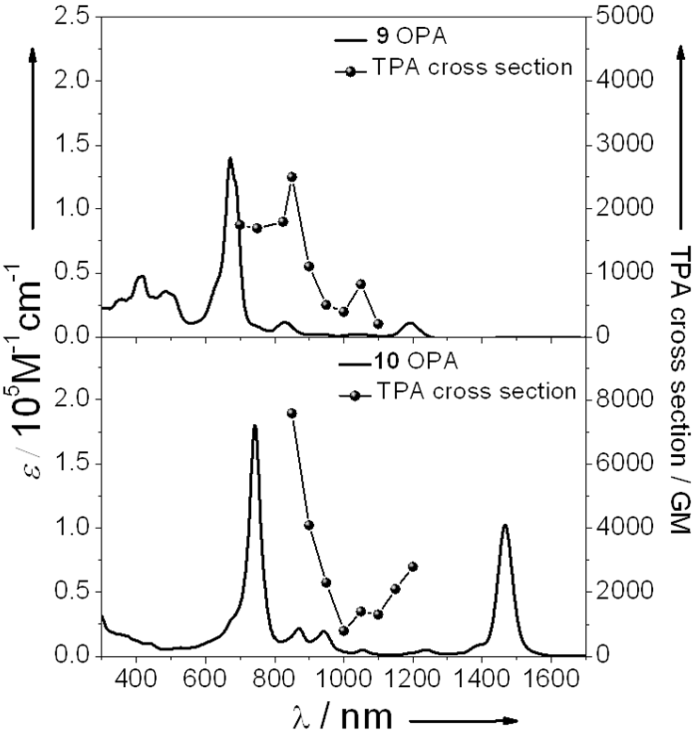

Figure 8. One- (OPA, solid line and left vertical axis) and two-photon absorption (TPA, symbols and right vertical axis) spectra of 9 (top), and 10 (bottom) measured in CH2Cl2. TPAspectra are plotted at $\lambda_{ex}/2$.

(c) A Möbius Antiaromatic Complex as a Kinetically Controlled Product in Phosphorus Insertion to a [32]Heptaphyrin

In recent years, the π-conjugation topology has become an important issue in discussing aromaticity of organic molecules, since quite a number of Möbius aromatic molecules have been actually explored, in which the 4nπ-electronic macrocyclic conjugation is attained along a singly twisted one-sided topology like a Möbius strip (so-called Möbius topology). The concept of Möbius aromaticity first proposed by Heilbronner in 1964 is complementary to the usual Hückel aromaticity by predicting that the [4n]π and [4n+2]π rule for aromaticity of the usual two-sided topology (so-called Hückel topology) should be reversed for macrocyclic molecules of Möbius topology. *meso*-Aryl expanded porphyrins have emerged as an effective platform to realize Möbius aromatic systems owing to their conjugated nature, conformational flexibilities, and facile capture and release of two pyrrolic protons upon two-electron oxidation and reduction, respectively.

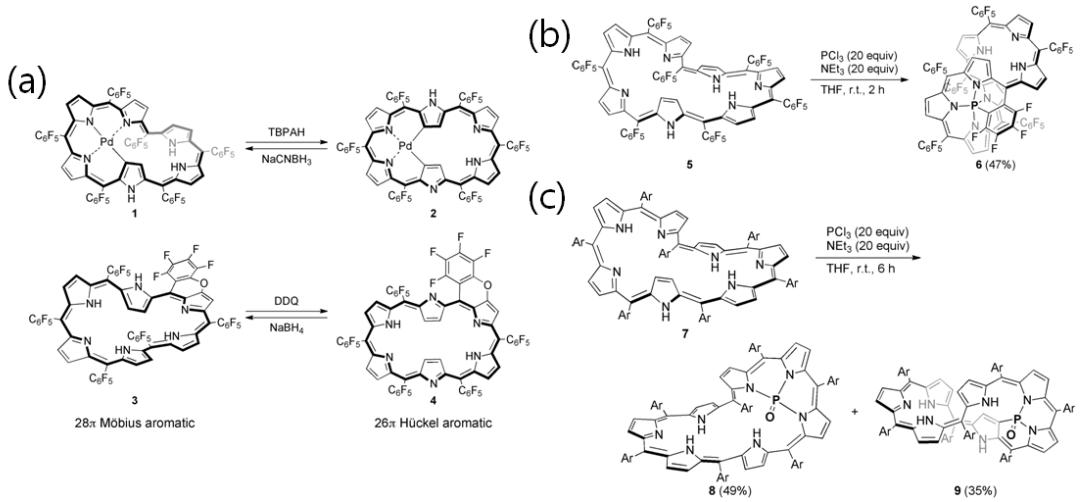

Scheme 2. (a) Previous attempts for Möbius antiaromatic species. (TBPAH = tris (4-bromophenyl) aminium hexachloroantimonate) (b) Synthesis of phosphorus complex **6** (c) Synthesis of phosphorus complexes **8** and **9**. (Ar = 2,6-dichlorophenyl)

Despite the increasing number of [4n]π Möbius aromatic molecules, [4n+2]π Möbius antiaromatic molecules still remain very rare. This is not surprising; since Möbius antiaromatic molecules are unfavourable with respect to electronic delocalization associated chemical stability and structural distortion. As a rare example, Latos-Grażyński et al. reported a cationic palladium(II) complex of [18]vacataporphyrin that exhibited a weak paratropic ring current. We have explored a bis-phosphorus complex of [30]hexaphyrin,

which has, to the best of our knowledge, constituted the only example of a structurally well-characterized Möbius antiaromatic molecule. As shown in Scheme 2, our attempts to form Möbius antiaromatic [26]hexaphyrins by the oxidations of Möbius aromtic [28]hexaphyrins **1** and **3** failed, merely producing Hückel aromatic [26]hexaphyrins **2** and **4** via topology switch. Putative Möbius antiaromatic [26]hexaphyrins were not detected. Herein, we report that phosphorus insertion to [32]heptaphyrin led to the formation of a Möbius antiaromatic phosphorus complex of [34]heptaphyrin, **8** as a kinetically controlled product, which thermally rearranged to a more stable Hückel aromatic complex, **9**, quantitatively (Scheme 2). *meso*-Aryl-substituted heptaphyrins(1.1.1.1.1.1.1) show versatile reactivities and properties, while usually taking their 32π oxidation states as the most stable forms.

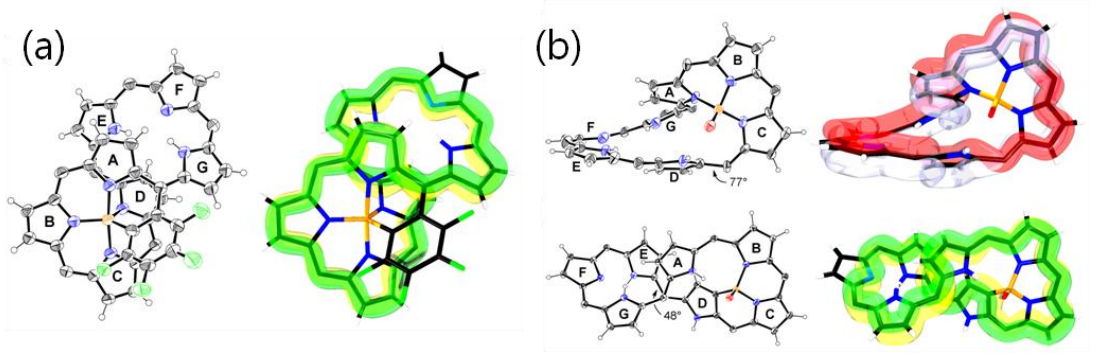

Figure 9. (a) X-Ray crystal structure and schematic representation of the molecular orbital of **6**. Thermal ellipsoids represent 30% probability. *meso*-Aryl substituents and solvent molecules are omitted for clarity. (b) X-Ray crystal structure (left) and schematic representation of the molecular orbital (right) of (a) **8** and (b) **9**. Thermal ellipsoids represent 30% probability. *meso*-Aryl substituents and solvent molecules are omitted for clarity. Dihedral angles at the most distorted poins are given.

Our studies on the phosphorus insertion into *meso*-aryl expanded porphyrins have revealed that the coordinated phosphorus atoms exists as a P(V) state either in a phosphoramide or penta-coordinated form, stabilizing reduced oxidation-states of expanded porphyrins. We thus envisioned that [34]heptaphyrins may be generated by the phosphorus insertion into heptaphyrins, while such heptaphyrin have been quite exceptional so far besides a quadruplly *N*-fused heptaphyrin. The phosphorus atom is penta-coordinated, being bound to the four nitrogen atoms of pyrrole A, B, C and D, and the *ortho*-carbon atom of *meso*-pentafluorophenyl group in a trigonal bipyramidal manner. The ^{1}H NMR spectrum exhibits two signals at 13.73 and 13.61 ppm due to the NH protons and fourteen signals in the range of 8.08–5.07 ppm due to the pyrrolic *β*-protons and the ^{31}P NMR shows a signal at –82.41 ppm, which is in the range of penta-coordinated phosphorus atoms with the same

coordination geometry. The complex **6** can be regarded as a weak Hückel aromatic molecule, which is supported by its absorption spectrum and small but negative NICS values. This structure, combined with its 34π-electronic network, tempted us to regard this as a Möbius antiaromatic molecule. This is indeed the case, since 1) the UV/vis absorption spectrum of **8** has an ill-defined Soret-like band and weak and broad bands in near-IR region, which are characteristic of antiaromatic expanded porphyrins (Figure 10), and 2) the ^{1}H NMR spectrum of **8** characteristically displays signals due to the inner (almost lateral) pyrrolic *β*-protons in the pyrrole rings A and D at 7.96 and 7.60 ppm, which are distinctly deshielded from the other outer *β*-protons that appear in the range of 6.51–5.51 ppm (Figure 11), indicating a weak paratropic ring current. In line with this, the inner NH protons in the pyrroles E and G appear at 12.59 and 11.42 ppm, which are also deshielded as compared with the outer one in the pyrrole D at 10.14 ppm. The difference between the chemical shifts of the most shielded and most deshielded *β*-protons is only –2.45 ppm.

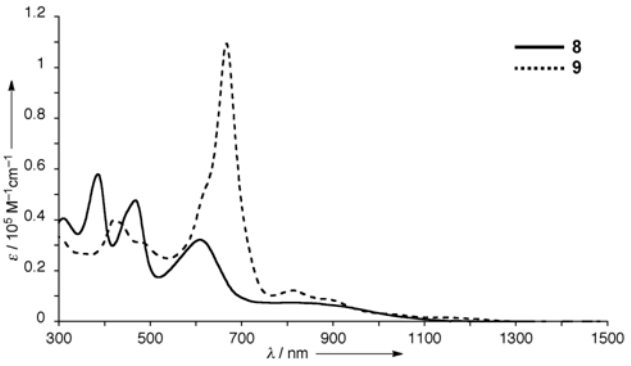

Figure 10. UV/Vis absorption spectra of **8** and **9** in CH_2Cl_2.

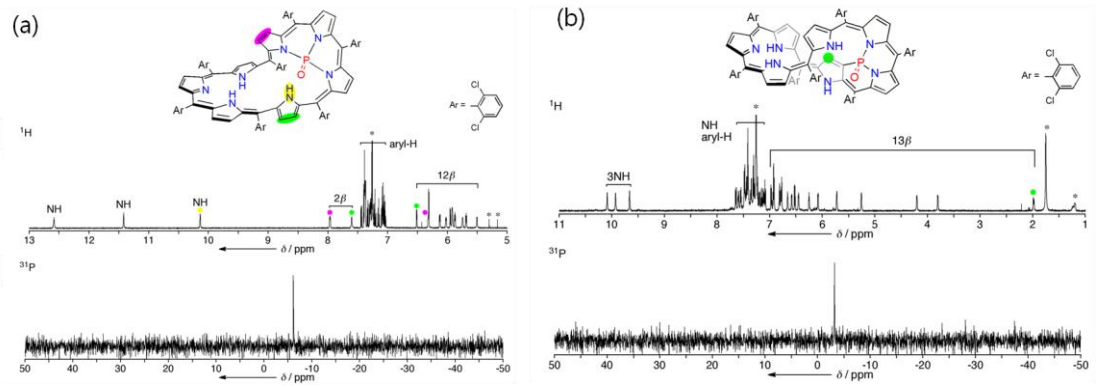

Figure 11. ^{1}H NMR spectra of (a) **8** at 25 ℃ and (b) **9** at –60 ℃ in $CDCl_3$. Peaks marked with * arise from residual solvents and impurities.

The weaker paratropic ring current of **8** as compared with that of Möbius antiaromatic phosphorus complex of [30]hexaphyrin **10** (–5.60 ppm and the largest dihedral angle is 67°),

can be ascribed to the larger largest dihedral angle. The other complex **9** has been determined to take a figure-eight, double-sided (Hückel) structure on the basis of X-ray diffraction analysis (Figure 9).

The P=O moiety is bound to the two nitrogen atoms of the pyrroles B and C, and the *β*-carbon atom of the pyrrole D. The complex **9** has been assigned as a 34π-Hückel aromatic molecule. The UV/vis absorption spectrum of **9** exhibits an intense Soret-like band at 667 nm and Q-band like bands at 813, 892, and 1157 nm (Figure 10), which are characteristic of the aromatic porphyrinoids. The ^{1}H NMR spectrum of **9** is very broad at room temperature, probably due to conformational flexibility, but became sharpened at –60 ℃, exhibiting a doublet at 1.98 ppm due to the inner *β*-proton in the pyrrole D adjacent to the P=O moiety and twelve signals due to the other *β*-protons in a range of 6.91–3.80 ppm (Figure 11), The chemical shift difference is relatively large, +4.93 ppm, indicating the presence of a certain diatropic ring current. The complex **8** underwent two reversible reductions at –1.55 and –1.92 V and two reversible oxidations at –0.17 and 0.07 V, while the complex **9** showed one reduction wave at –1.89 V and two oxidation waves at –0.34 and 0.08 V all as reversible processes. The electrochemical HOMO–LUMO gaps were thus calculated to be 1.38 and 1.55 eV for **8** and **9**, respectively. The smaller HOMO–LUMO gap of **8** is in line with its assignment as an antiaromatic species.

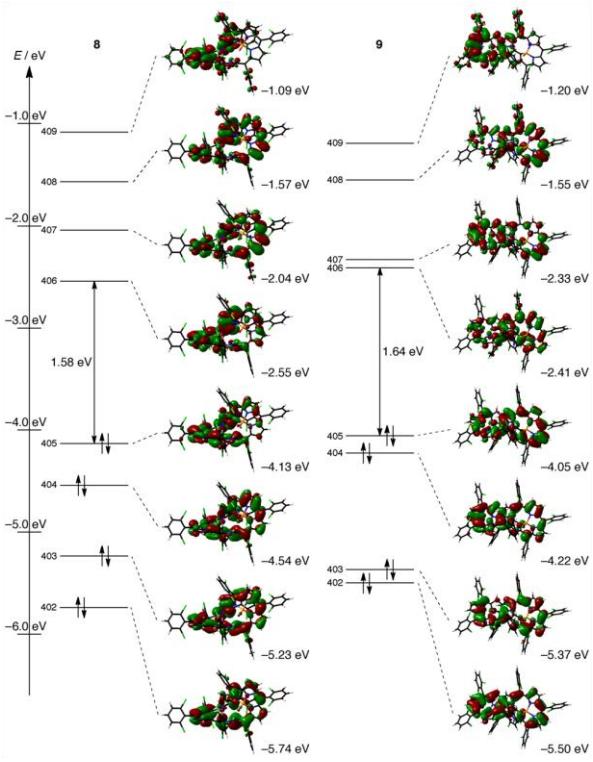

Figure 12. Selected molecular orbitals of **8** and **9** on the optimized structures.

In order to obtain the information on **8** and **9**, we performed theoretical calculation at RB3LYP/6-31G(d) level on the basis of the optimized structures by using Gaussian program (Figure 12). Importantly, the total energy of **8** has been calculated to be as much as 31.0 kcal/mol higher than that of **9**. HOMO-LUMO gaps have been calculated to be 1.58 and 1.64 eV for **8** and **9**, respectively. Time-dependent DFT calculation predicts a weak

absorption band around 1037 nm for **8** and an intense Soret-like band at 630 nm for **9**, which are respectively characteristic features of antiaromatic and aromatic expanded porphyrins.

Interestingly, the yields of **8** and **9** were temperature dependent; 33 and 17% with the recovery of **7** (45%) in the reaction at 0 ℃ for 3 h and 18 ad 74% at 60 ℃ for 3 h. More directly, we examined the thermal conversion of **8** to **9** that involved the phosphoramide rearrangement with a topology change from Möbius to Hückel. While rather stable toward heating at 60 ℃ in THF, $CHCl_3$, and acetone, heating of **8** in acetonitrile at 60 ℃ for 12 h gave rise to the quantitative transformation to **9**. These changes were clearly traced by UV-vis spectroscopy. The rate of this conversion were determined by monitoring the increasing absorbance of **9** at 622 nm at various temperature to be 2.2×10^{-6} s^{-1} at 60 ℃, 3.9×10^{-6} s^{-1} at 65 ℃, 4.6×10^{-6} s^{-1} at 70 ℃, 5.9×10^{-6} s^{-1} at 75 ℃, and 9.3×10^{-6} s^{-1} at 80 ℃. On the basis of these results, the activation parameters of the isomerization have been determined as the following: activation energy, E_a = 65.3 kJ mol^{-1}; activation enthalpy, $H^{\ddagger}$ = 62.4 kJ mol^{-1}; and activation entropy, $S^{\ddagger}$ = –166 J mol^{-1}. Thus, these results indicate that **8** is a kinetically controlled product that undergoes exothermic conversion to **9**.

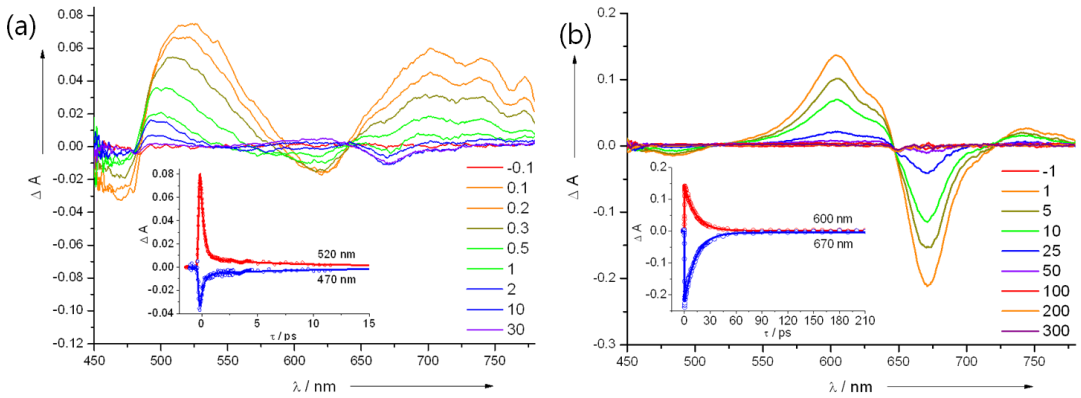

Figure 13. Transient absorption spectra of (a) **8** and (b) **9** on the optimized structures. The inset shows the decay profiles.

The aromaticity of expanded porphyrins is prominently distinguished in time-resolved spectroscopic measurements. The aromatic molecule **9** shows the distinct excited-state properties of aromatic expanded porphyrins. Typically, we have observed that the differential absorption spectra of aromatic expanded porphyrins show strong ground-state bleaching (GSB) signals with relatively weak excited-state absorption (ESA) signals. These signals are also seen in the transient absorption spectra of **9**. In contrast, the spectra of **8** show small GSB and large ESA signals, and are quite different from those of **9**. These

spectral features, together with faster decay dynamics of **8** than **9**, are unique for antiaromatic expanded porphyrins. The difference in excited-state dynamics between aromatic and antiaromatic expanded porphyrins could be mainly attributed to the different electronic structures of these two classes of molecules. The perturbed degeneracy of HOMO/HOMO-1 and LUMO/LUMO+1 causes the interruption of two additional frontier MOs, thus resulting in a change in configuration interactions. As a consequence, the electronic transitions or states that affect the steady- and excited-state dynamics are perturbed. The presence of the optical dark state governs its photophysical behavior. Based on these results, the fast decay of **8** can be ascribed to the NIR dark state that acts as a ladder in the deactivation processes.

Summary

In this project, we have investigated the relationship between aromaticity and photophysical properties of various (anti)aromatic porphyrinoids using the spectroscopic techniques and theoretical approaches.

Firstly, Hybrid porphyrin tapes have been prepared and characterized and have been compared with their parent porphyrin tapes. X-ray crystal structures of porphyrin tape trimers 4 and 5 have been reported for the first time. Hybrid porphyrin tapes have been shown to be more soluble and more chemically stable. The TPA value for the trimer 2 was measured to be 21 000 GM, which is much larger than that of the dimer 1, reflecting that the TPA values are strongly associated with p-conjugation length. The TPA values of hybrid porphyrin tapes 3-6 bearing an acceptor-type porphyrin unit were measured to be 2200, 27000, 24000, and 26000 GM, respectively. These results indicate that the donor-acceptor-donor strategy slightly but definitely improves the overall TPA properties, although the effect of p-conjugation is a dominant contribution to the enhancement of TPA properties. This work will help further design of molecules with large TPA properties.

Secondly, bis(AuIII) complex **10**, containing a hexaphyrin fused to two anthracenes, was prepared and characterized. Owing to the flat and elongated rectangular conjugated network, **10** displays a remarkably red-shifted and sharp Q-band-like band at 1467 nm, higher reversible oxidation potentials, multicharge storage ability, and a large TPA cross-section value. Hence, this work demonstrates the utility of [26]hexaphyrin as an electronically more-flexible unit to create extensively π-conjugated networks.

Thirdly, Möbius antiaromatic [34]heptaphyrin **8** was isolated as a stable product in the phosphorus insertion reaction of [32]heptaphyrin **7**. Möbius antiaromatic character of **8** has been indicated by its X-ray structure, weak paratropic ring current, ultrafast excited state dynamics and ill-defined absorption features. The complex **8** is highly strained and is quantitatively converted to more stable double-twisted Hückel aromatic [34]heptaphyrin **9** with the migration of the P=O moiety from NNN to NNC upon heating in acetonitrile.

References

(1) J. L. Sessler, A. Gebauer, S. J. Weghorn, in *The Porphyrin Handbook*, Vol. 2 (eds. K. M. Kadish, K. M. Smith, R. Guilard), Academic Press, New York, **2000**, ch. 9.

(2) J. L. Sessler, S. Camiolo, P. A. Gale, *Coord. Chem. Rev.* **2003**, *240*, 17.

(3) A. Srinivasan, H. Furuta, *Acc. Chem. Res.* **2005**, *38*, 10.

(4) R. Misra, T. K. Chandrashekar, *Acc. Chem. Res.* **2008**, *41*, 265.

(5) A. Kay, M. Grätzel, *J. Phys. Chem.* **1993**, *97*, 6272.

(6) L. Schmidt-Mende, W. M. Campbell, Q. Wang, K. W. Jolley, D. L. Officer, Md. K. Nazeeruddin, M. Grätzel, *ChemPhysChem* **2005**, *6*, 1253.

(7) M. Stępień, L. Latos-Grażyński, N. Sprutta, P. Chwalisz, L. Szterenberg, *Angew. Chem. Int. Ed.* **2007**, *46*, 7869.

(8) Y. Tanaka, S. Saito, S. Mori, N. Aratani, H. Shinokubo, N. Shibata, Y. Higuchi, Z. S. Yoon, K. S. Kim, S. B. Noh, J. K. Park, D. Kim, A. Osuka, *Angew. Chem. Int. Ed.* **2008**, *47*, 681.

(9) E. Heilbronner, *Tetrahedron Lett.* **1964**, *5*, 1923.

(10) J. Garratt, *Aromaticity*, John Wiley & Sons, Inc., New York, **1986**.

(11) V. I. Minkin, M. N. Glukhotsev, B. Y. Simkin, *Aromaticity and Antiaromaticity: Electronic and Structural Aspects*, John Wiley & Sons, Inc., New York, **1994**.

(12) H. S. Rzepa, *Chem. Rev.* **2005**, *105*, 3697.

(13) R. Herges, *Chem. Rev.* **2006**, *106*, 4820.

(14) K. B. Wiberg, *Chem. Rev.* **2001**, *101*, 1317.

(15) Z. S. Yoon, A. Osuka, D. Kim, *Nature Chem.* **2009**, *1*, 113.

(16) B. Lament, J. Dobkowski, J. L. Sessler, S. J. Weghorn, J. Waluk, *Chem. Eur. J.* **1999**, *10*, 3039.

(17) M. K. Cyranski, T. M. Krygowski, M. Wisiorowski, N. J. R. van E. Hommes, P. von R. Schleyer, *Angew. Chem. Int. Ed.* **1998**, *37*, 177.

(18) H.-E. Song, J. A. Cissell, T. P. Vaid, D. Holten, *J. Phys. Chem. B*, **2007**, *111*, 2138.

List of Publications

1. Donor-Substituted β-Functionalized Porphyrin Dyes on Hierarchically-Structured Mesoporous TiO_2 Spheres. Highly Efficient Dye-Sensitized Solar Cells
Masatoshi Ishida , Sun Woo Park , Daesub Hwang , Young Bean Koo , Jonathan L. Sessler , Dong Young Kim , and Dongho Kim
The Journal of Physical Chemistry C, **2011**, *115* (39), 19343–19354

2. Neutral Radical and Singlet Biradical Forms of meso-Free, Keto, and Diketo Hexaphyrins(1.1.1.1.1.1): Effects on Aromaticity and Photophysical Properties
Masatoshi Ishida, Jae-Yoon Shi , Jong Min Lim , Byung Sun Lee , Min-Chul Yoon , Taro Koide , Jonathan L. Sessler , Atsuhiro Osuka , and Dongho Kim
Journal of the American Chemical Society, **2011**, *133* (39), 15533–15544

3. Ion-Controlled On–Off Switch of Electron Transfer from Tetrathiafulvalene Calix[4]pyrroles to $Li^+@C_{60}$
Shunichi Fukuzumi, Kei Ohkubo, Yuki Kawashima, Dong Sub Kim, Jung Su Park, Atanu Jana, Vincent M. Lynch, Dongho Kim, and Jonathan L. Sessler
Journal of the American Chemical Society, **2011**, *133*(40), 15938-15941

4. π-Extension in Expanded Porphyrins: Cyclo[4]naphthobipyrrole
Vladimir V. Roznyatovskiy, Jong Min Lim, Vincent M. Lynch, Byung Sun Lee, Dongho Kim, and Jonathan L. Sessler
Organic Letters, **2011**, *13(*20), 5620-5623

5. Comparative Photophysical Properties between Bicyclo[2.2.2]octadiene (BCOD)- and Benzo-Fused Free-Base Triphyrins (2.1.1)
Young Mo Sung, Jong Min Lim, Zhaoli Xue, Zhen Shen and Dongho Kim
Chem. Commun., **2011**, *47*(47), 12616-12618.

6. Solvent- and Temperature-Dependent Conformational Changes between Hückel Antiaromatic and Möbius Aromatic Species in meso Trifluoromethyl-Substituted [28]Hexaphyrins
Min-Chul Yoon , Pyosang Kim , Hyejin Yoo , Soji Shimizu , Taro Koide , Sumito Tokuji , Shohei Saito , Atsuhiro Osuka, Dongho Kim
J. Phys. Chem. B, **2011**, *115(*50), 14928-14937

7. Synthesis and Properties of Hybrid Porphyrin Tapes
Takayuki Tanaka, Byung Sun Lee, Naoki Aratani, Min-Chul Yoon, Dongho Kim, Atsuhiro Osuka
Chem. Eur. J., **2011**, *17*(51), 14400-14412.

8. Mesomorphic Organization and Thermochromic Luminescence of Dicyanodistyrylbenzene-8Based Phasmidic Molecular Disks: Uniaxially Aligned Hexagonal Columnar Liquid Crystals at Room Temperature with Enhanced Fluorescence Emission and Semiconductivity
Seong-Jun Yoon, Jong H. Kim, Kil Suk Kim, Jong Won Chung, Benoît Heinrich, Fabrice Mathevet, Pyosang Kim, Bertrand Donnio, André-Jean Attias, Dongho Kim and Soo Young Park
Adv. Funct. Mater. (Advanced Functional Materials), **2012**, *22* (1), 61–69

9. Single-Molecule Fluorescence Dynamics of Butadiyne-Linked Porphyrin Dimer: Effect of Conformational Flexibility in Host Polymers
Ji-Eun Lee, Jaesung Yang and Dongho Kim
Faraday Discuss. (Faraday Discussions), **2012,** *155* (1), 277-288

10. Polymer Matrix Dependence of Conformational Dynamics within a π-Stacked Perylenediimide Dimer and Trimer Revealed by Single Molecule Fluorescence Spectroscopy
Hyejin Yoo, Hee Won Bahng, Michael R. Wasielewski and Dongho Kim
Phys. Chem. Chem. Phys., **2012**, *14*(6), 2001-2007
Physical Chemistry Chemical Physics

11. Ensemble and Single-Molecule Spectroscopic Study on Excitation Energy Transfer Processes in 1,3-Phenylene-Linked Perylenebisimide Oligomers
Hee Won Bahng, Min-Chul Yoon, Ji-Eun Lee, Yuichi Murase, Tomoki Yoneda, Hiroshi Shinokubo, Atsuhiro Osuka, and Dongho Kim
J. Phys. Chem. B, **2012**, *116*(4), 1244–1255

12. Cyclo[m]pyridine[n]pyrroles: Hybrid Macrocycles That Display Expanded π-Conjugation upon Protonation
Zhan Zhang, Jong Min Lim, Masatoshi Ishida, Vladimir V. Roznyatovskiy, Vincent M. Lynch, Han-Yuan Gong, Xiaoping Yang, Dongho Kim, and Jonathan L. Sessler
J. Am. Chem. Soc., **2012**, *134*(9), 4076-4079.

13. Synthesis, Characterization, and Spectroscopic Analysis of Antiaromatic Benzofused Metalloporphyrins
Shun Sugawara, Yusuke Hirata, Satoshi Kojima, Yohsuke Yamamoto, Eigo Miyazaki, Kazuo Takimiya, Shiro Matsukawa, Daisuke Hashizume, John Mack, Nagao Kobayashi, Zhen Fu, Karl M. Kadish, Young Mo Sung, Kil Suk Kim and Dongho Kim
Chem. Eur. J., **2012**, *18*(12), 3566–3581

14. Molecular Engineering and Solvent Dependence of Excitation Energy Hopping in Self-Assembled Porphyrin Boxes
Hee Won Bahng, Pyosang Kim, Young Mo Sung, Chihiro Maeda, Atsuhiro Osuka and Dongho Kim
Chem. Commun., **2012**, *48(*35), 4181-4183

15. Electrochemical Synthesis of a Thiophene-Containing Cyclo[9]pyrrole
Thanh-Tuan Bui, Adriana Iordache, Zhongrui Chen, Vladimir V. Roznyatovskiy, Eric Saint-Aman, Jong Min Lim, Byung Sun Lee, Sudip Ghosh, Jean-Claude Moutet, Jonathan L. Sessler, Dongho Kim and Christophe Bucher
Chem. Eur. J., **2012** *18*(19), 5853-5859 20120507

16. Synthesis of Stable Monoporphyrinate Lanthanide(III) Complexes without Ancillary Ligand
Eui-Jong Kim, Pyosang Kim, Chi-Hwa Lee, Jooyoung Sung, Hongsik Yoon, Dongho Kim and Woo-Dong Jang
Chem. Commun., **2012**, *48*(45), 5611-5613

17. Low-Temperature Fabrication of TiO_2 Electrodes for Flexible Dye-Sensitized Solar Cells Using an Electrospray Process
Horim Lee, Daesub Hwang, Seong Mu Jo, Dongho Kim, Yongsok Seo, and **Dong Young Kim**
ACS Appl. Mater. Interfaces, 2012, *4*(6), 3308-3315

18. A Non-Fused Mono-*Meso*-Free Pentaphyrin and Its Rhodium(I) Complex
Tomoki Yoneda, Hirotaka Mori, Byung Sun Lee, Min-Chul Yoon, Dongho Kim and Atsuhiro Osuka
Chem. Commun., **2012**, 48(54), 6785-6787

19. Excitation Energy Transfer in Multiporphyrin Arrays with Cyclic Architectures: Towards Artificial Light-Harvesting Antenna Complexes
Jaesung Yang, Min-Chul Yoon, Hyejin Yoo, Pyosang Kim and Dongho Kim
Chem. Soc. Rev., **2012**, 41(14), 4808-4826

20. Excitation Energy Migration Processes in Various Multi-Porphyrin Assemblies
Jaesung Yang, Dongho Kim
Philosophical Transactions of the Royal Society A (ISSN: 1364-503X)
Phil. Trans. R. Soc. A **2012**, 370, 3802-3818

21. Tetrakis(4-*tert*-butylphenyl) substituted and fused quinoidal porphyrins
Wangdong Zeng, Byung Sun Lee, Young Mo Sung, Kuo-Wei Huang, Yuan Li, Dongho Kim and Jishan Wu
Chem. Commun., **2012**, 48(62), 7684-7686.

22. An Electron-Deficient Porphyrin Tape
Hirotaka Mori, Takayuki Tanaka, Naoki Aratani, Byung Sun Lee, Pyosang Kim, Dongho Kim and Atsuhiro Osuka
Chem. Asian J., **2012**, 7(8), 1811-1816.

23. Excitation Energy Migration in Covalently Linked Perylene Bisimide Macrocycles
Felix Schlosser, Jooyoung Sung, Pyosang Kim, Dongho Kim, Frank Würthner
Chem. Sci., **2012**, *3*(9), 2778-2785

24. Synthesis and Recognition Properties of Higher Order Tetrathiafulvalene (TTF) Calix[n]pyrroles (n = 4-6)
Jung Su Park, Christopher Bejger, Karina R. Larsen, Kent A. Nielsen, Atanu Jana, Vincent M. Lynch, Jan O. Jeppesen, Dongho Kim, and Jonathan L. Sessler
Chem. Sci., **2012**, *3*(9), 2685-2689

25. The Role of Nitrogen Bridges Perturbing the Photophysical Properties in the Porphyrin Framework
Young Mo Sung, Ewa Pacholska-Dudziak, Lechosław Latos-Grażyński and Dongho Kim
Chem. Commun., **2012**, *48*(69), 8643-8645

26. Hexaphyrin Fused to Two Anthracenes
Koji Naoda, Hirotaka Mori, Naoki Aratani, Byung Sun Lee, Dongho Kim, and Atsuhiro Osuka
Angew. Chem. Int. Ed. **2012**, 124,

DD882: As a separate document, please complete and sign the inventions disclosure form.

This document may be as long or as short as needed to give a fair account of the work performed during the period of performance. There will be variations depending on the scope of the work. As such, there is no length or formatting constraints for the final report. Include as many charts and figures as required to explain the work. A final report submission very similar to a full length journal article will be sufficient in most cases.